Bull. Mater. Sci. (2020) 43:120
https://doi.org/10.1007/s12034-020-2084-x

Effect of transition metal doping on Cr–Ru alloys using first principles approach

B O MNISI[1,*], E M BENECHA[1], H R CHAUKE[2], P E NGOEPE[2] and M M TIBANE[1]
[1]College of Science, Engineering and Technology, University of South Africa, Science Campus, Roodepoort 1709, South Africa
[2]Materials Modelling Centre, University of Limpopo, Private Bag X1106, Sovenga 0727, South Africa
*Author for correspondence (bhila.oliver00@gmail.com)

MS received 22 October 2019; accepted 16 December 2019

Abstract. *Ab-initio* density functional theory calculations have been used to explore the effect of transition metal alloying on A15 Cr–Ru intermetallic alloys. We study the structural, electronic and mechanical properties of Ru_3Cr and Cr_3Ru alloys doped with transition metals (M = Mn, Mo, Pt, Pd, Fe, Co, Re and Zr). Their thermodynamic and mechanical behaviours were deduced from the heat of formation, ratio of bulk to shear modulus, density of states (DOS) as well as elastic constants predictions. We find that Mn doping in these alloys leads to thermodynamic stability. These compounds also show a valence–conduction band overlap around the Fermi energy as depicted by the DOS. Furthermore, the Pugh ratio (the ratio of bulk to shear modulus) indicates the ductility character of these compounds. Their mechanical stability was illustrated by the Bohr mechanical stability criteria with all the elastic constants having a value >0. These results demonstrate that these systems can potentially be used as coating materials in high temperature structural applications.

Keywords. A15 Cr–Ru alloys; transition metal doping; density functional theory; structural properties; stability; high-temperature alloys.

1. Introduction

Chromium-based alloys are earmarked as possible coating materials in various technological industries due to their exceptional physical and corrosion resistance properties [1]. Particularly, chromium-based alloys are currently used as coating materials in elevated temperature environments, such as gas turbine engines, where hot corrosion and oxidation are prevalent. These environmental hazards reduce the performance and life-span of the gas turbine engines [1]. However, chromium-based alloys suffer from low adhesion to the substrate, porosity and low resistance to electron flow in the coating layer. Nickel-based super alloys (NBSAs) have previously been suggested as alternative coating materials due to their high melting point (1455°C), high corrosion resistance and oxidation, as well as low density. Despite the success of the NBSAs, they are presently at the limit of their high-temperature capability [1]. Hence there is need to search for alternative materials to replace the currently used NBSAs in high temperature structural applications. Platinum-based alloys have been suggested [2] as potential alternatives to NBSAs owing to their noble corrosion resistance and high melting points. Although platinum has a high melting temperature than nickel its application is limited by its high cost and higher density.

Recently, Cr–Ru based alloys have attracted interest in high temperature structural applications due to the relatively high melting temperature of Cr (1907°C) and Ru (2334°C) as well as excellent oxidation and corrosion resistance. However, the Cr–Ru alloys are deprived by their low diffusion rate and easy oxidation in air. Therefore, Cr–Ru system has limited thermodynamical data [3,4], hence research to enhance their applicability in high temperature industrial applications has continued unabated. In Ru–Cr phase diagram, Cr_3Ru, Cr_2Ru and Cr_4Ru phases exist experimentally in their respective temperature formations [5,6], while the diffraction patterns of Cr_4Ru and the Cr_7C_3 phase have been reported by Wopersnow and Raub [7]. Also, a narrow homogeneity range of 31.5 atm% Ru and 32–36 atm% Ru for A15 Cr_3Ru and Cr_2Ru (σ phase) have been identified by Venkatraman and Neumann [8], respectively in the Cr–Ru phase diagram. Further, the A15 Cr_3Ru phase has been found to exist at temperatures ranging between 750 and 1000°C [7]. Experimental work has been carried out previously on Pt–Cr–Ru ternary alloys to understand the origin of phases occurring within it [4,9,10]. An isothermal section of Pt–Cr–Ru alloy was found in Pd–Pt–Rh–Ru–Cr system using micro-analytical and diffusion multiple techniques like electron backscatter diffraction (EBSD) at 1200°C [11], while Süss *et al* [6] found a solidification projection of Pt–Cr–Ru alloy instead of the isothermal section at 1200°C. Further, a primary isothermal section of Ni–Cr–Ru ternary system at 1000 and 1250°C was described by Chakravorty and West [9].

Published online: 30 April 2020

In this work, we study the effect of transition metal dopants on the stability of A15 Ru–Cr binary systems. Specifically, we explore the stability of Ru–Cr–M (M = V, Pt, Pd, Co, Re, Mo, Fe, Mn and Zr) by examining the heat of formation, the electron density of states (DOS) and elastic constants. Our results indicate that incorporation of these transitions metal dopants significantly enhances the stability of Ru–Cr alloys. Moreover, we have established that B/G ratio of the Cr–Ru–M systems is above 1.75, suggesting ductility of the materials.

2. Computational details

The *ab-initio* plane wave (PW) pseudopotential nonspin polarized density functional theory calculations as embodied in the CASTEP code [10] was used to determine the stability, electronic structure and mechanical properties of Ru–Cr–M binary alloys. Description of electronic exchange-correlation was treated by the Perdew–Burke–Ernzerhof generalized gradient approximation (GGA) functional [12,13], while the Vanderbilt ultra-soft pseudopotential [14] was employed for valence–core interactions. To study the effect of transition metal doping in the Cr–Ru–M ternary alloy systems, a $2\times2\times2$ supercell was constructed from optimized Cr–Ru unit cells. The PW basis set was defined by a well converged energy cut-off of 500 eV for all structures, while converged $4\times4\times4$ Monkhorst–Pack k-point sampling was used for integration over the Brillouin zone [15]. Similar set of k-points was used for the calculation of elastic constants and the DOS. A convergence criteria of 1×10^{-5} eV per atom, 0.03 eV Å^{-1} and 0.001 Å were used for the total energies, forces and structural displacement for geometry optimization calculations, respectively. The effect of transition metal (M = V, Pt, Co, Re, Mo, Fe, Mn and Zr) dopants on the stability, electronic and mechanical properties of Cr–Ru alloys was determined *via* substituting Ru with M atoms in A15 Ru_3Cr and Cr with M atoms in A15 Cr_3Ru supercells (figure 1), while considering various dopant concentrations of the transition metal atoms.

3. Results and discussion

3.1 *Structural and thermodynamic properties*

The lattice parameters and heat of formation of undoped binary A15 Ru_3Cr and A15 Cr_3Ru structures are calculated using both the LDA and GGA functionals, which are shown in table 1. The equilibrium GGA lattice parameters are found to be 4.777 and 4.623 Å, respectively, in agreement with previous theoretical data [16]. As expected, we find that LDA underestimates the lattice parameters for both the systems by 0.094 and 0.086 Å, respectively.

The heat of formation of the undoped intermetallic systems was calculated as:

$$\Delta H_{\mathrm{f}} = \left[\frac{E_{\mathrm{T}}(\mathrm{Cr,Ru}) - aE_{\mathrm{Cr}} - bE_{\mathrm{Ru}}}{a+b}\right], \tag{1}$$

while that of the doped systems was calculated as:

$$\Delta H_{\mathrm{f}} = \left[\frac{E_{\mathrm{T}}(\mathrm{Cr,Ru,M}) - aE_{\mathrm{Cr}} - bE_{\mathrm{Ru}} - cE_{\mathrm{M}}}{a+b+c}\right], \tag{2}$$

where $E_{\mathrm{T}}(\mathrm{Cr,Ru})$ and $E_{\mathrm{T}}(\mathrm{Cr,Ru,M})$ are total energies of the undoped and doped systems, respectively, while E_{Cr}, E_{Ru}, E_{M} are energies per atom of each atomic species, each containing number of atoms a, b and c, respectively. For the doped system, the atomic percentage contribution from each atom in the supercell for the Cr_3Ru and Ru_3Cr systems is given by $Cr_{0.75-x}Ru_{0.25}M_x$ and $Ru_{0.75-x}Cr_{0.25}M_x$, respectively, where x is the concentration of the metal dopant (M = Pt, Pd, Fe, Co, Mn, Re, Zr and V) calculated in the range of $0.01 \le x \le 0.09$.

From table 1, we find that the heat of formation of undoped Cr_3Ru and Ru_3Cr systems are positive (0.085 and 0.39 eV per atom, respectively), indicating that these systems are slightly unstable. Since previous studies [17] have shown that such systems may be stabilized upon doping, we have considered the effect of doping using various transition metal atoms including Pt, Pd, Fe, Co, Mn, Re, Zr and V. Figure 2 shows the calculated heat of formation of both $Ru_{0.75-x}Cr_{0.25}M_x$ and $Cr_{0.75-x}Ru_{0.25}M_x$ doped (M = Pt, Pd, Fe, Co, Mn, Re, Zr) for different dopant concentrations.

Generally, it is seen that the heat of formation for transition metal doped Ru-rich systems are higher than those of Cr-rich systems with the heat of formation decreasing with increasing dopant concentration in both the systems. An exception is observed in the case of Zr and Pd-doped Cr_3Ru at 0.08 and 0.09 atm% concentration and Mo-doped Ru_3Cr at 0.05 and 0.06 atm% concentrations. Notably, Mn-doped systems are the most stable in both the systems with the formation energy ranging from 0.14 to −0.59 eV per atom in Ru_3Cr and −0.079 to −0.75 eV per atom in Cr_3Ru at the considered dopant concentration range.

3.2 *Electronic properties*

The physical properties of materials are known to influence their electronic structure, and therefore, analysis of the electronic properties can be used to predict various properties of novel materials. In particular, the DOS, defined as the number of electronic states at a particular energy level that electrons are allowed to occupy, is closely related to the type of bonding (and hence, stability) of a material [18,19]. A structure is defined as being stable if the DOS fall exactly on the pseudogap at the Fermi energy level, whereas the system is unstable when the DOS fall on a peak or the anti-bonding side of the pseudogap [20–22].

Table 1. Calculated lattice constants and heat of formation of A15 Ru_3Cr and Cr_3Ru structures.

System	Prototype	a (Å) LDA	a (Å) GGA	a (Å) Previous work	ΔH_f (eV per atom) This work	ΔH_f (eV per atom) Previous work
Ru_3Cr	Cr_3Si	4.694	4.777	4.788	0.39	0.3225 [17]
Cr_3Ru	Cr_3Si	4.537	4.623	4.613 [16]	0.085	0.080 [16]

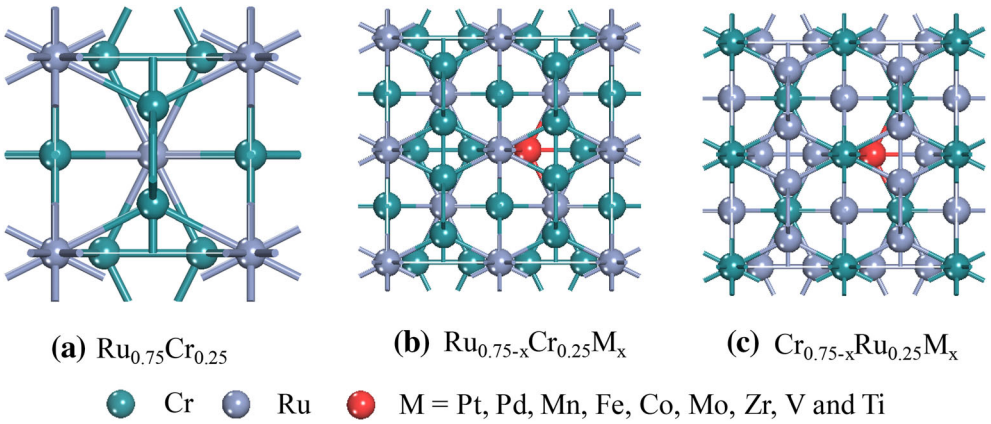

Figure 1. Illustration of the atomic arrangement showing (**a**) bulk A15 $Ru_{0.75}Cr_{0.25}$ undoped unit cell, (**b**) $2 \times 2 \times 2$ supercell of A15 $Ru_{0.75-x}Cr_{0.25}M_x$ and (**c**) $2 \times 2 \times 2$ supercell of A15 $Cr_{0.75-x}Ru_{0.25}M_x$, where M = Pt, Pd, Mn, Fe, Co, Mo, Zr, V and Zr and $0 \leq x \leq 0.09$ is the atomic concentration of the dopant.

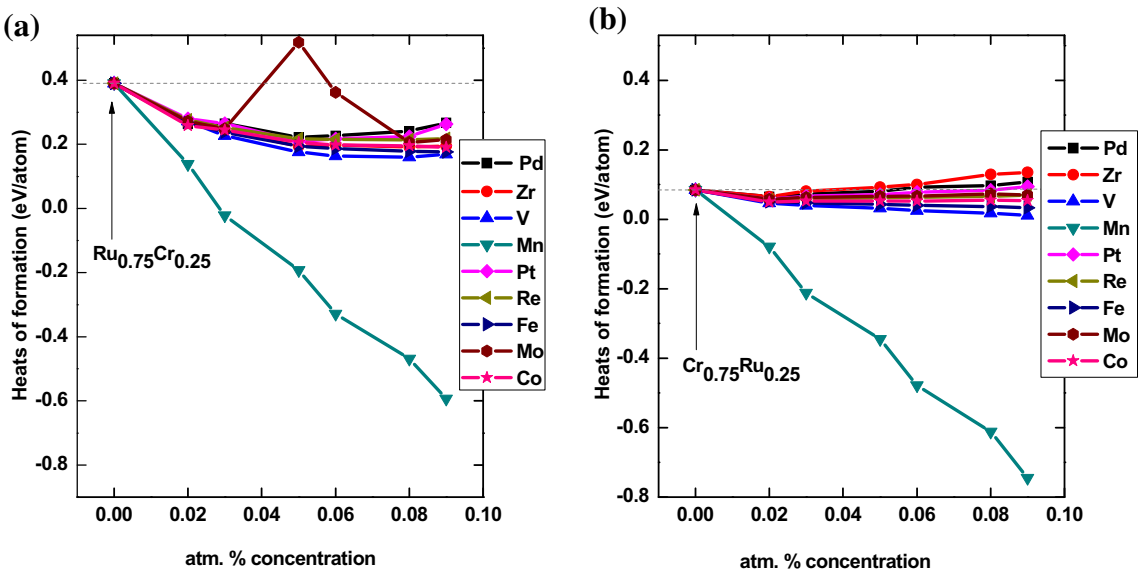

Figure 2. Calculated heat of formation as a function of dopant concentration for (**a**) $Ru_{0.75-x}Cr_{0.25}M_x$ and (**b**) $Cr_{0.75-x}Ru_{0.25}M_x$ (M = Pd, Zr, V, Mn, Pt, Re, Fe, Mo, Co) for $(0.00 \leq x \leq 0.09)$.

In figure 3, we show the DOS for the undoped and Fe, Mn and Mo-doped Cr-rich (Cr_3Ru) and Ru-rich (Ru_3Cr) systems. In both the systems, it is seen that there is a strong overlap of the conduction and valence bands, indicating the systems are metallic. Importantly, we find a significant change of the electronic properties of the Cr_3Ru and Ru_3Cr systems upon doping. We observe that the DOS of Cr_3Ru is characterized by sharp peaks, while those of Ru_3Cr are relatively

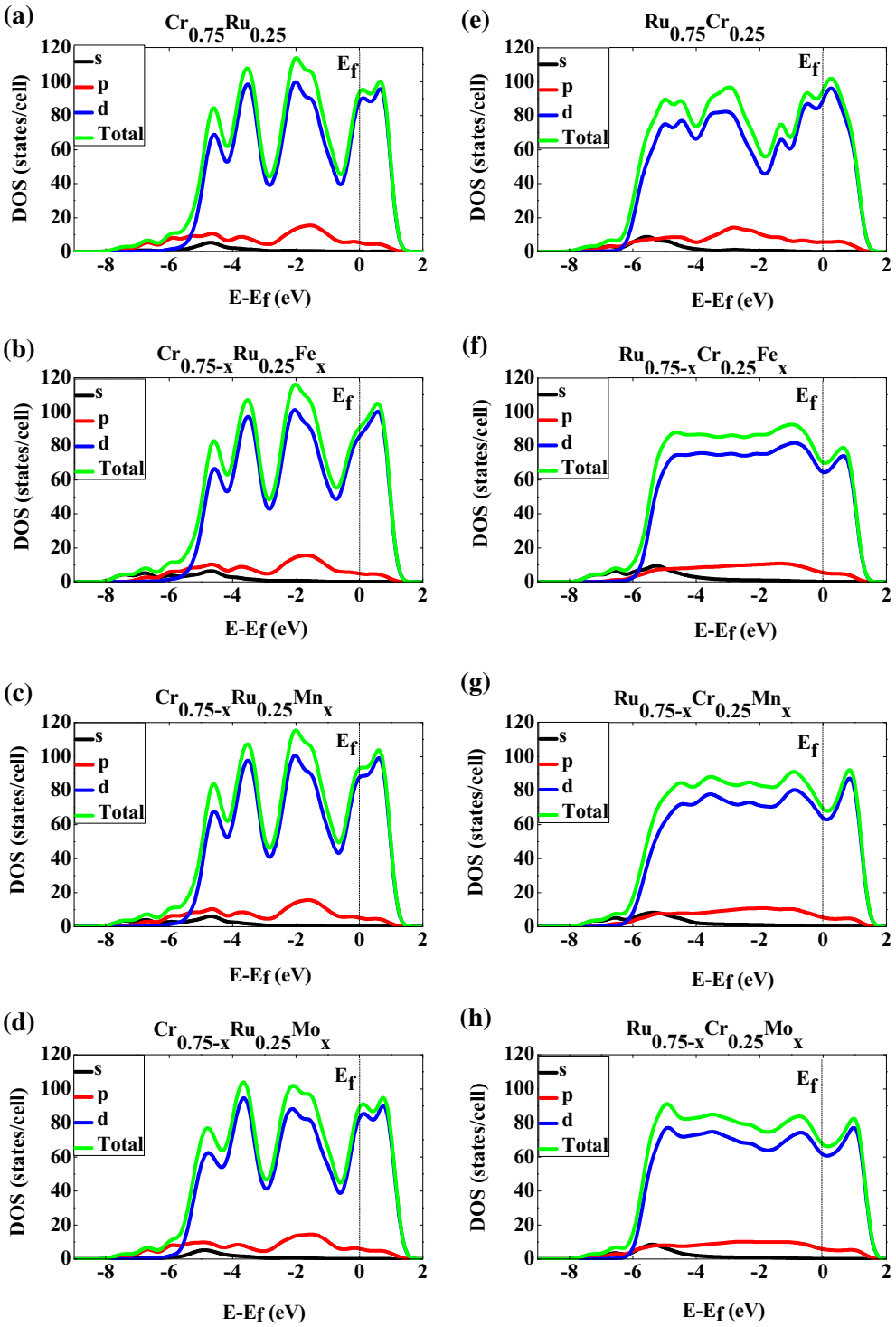

Figure 3. Calculated total and partial density of states (PDOS) for undoped (**a**) $Cr_{0.75}Ru_{0.25}$, doped (**b**) $Cr_{0.75-x}Ru_{0.25}Fe_x$, (**c**) $Cr_{0.75-x}Ru_{0.25}Mn_x$ and (**d**) $Cr_{0.75-x}Ru_{0.25}Mo_x$ chromium-rich alloys; (**e**) $Ru_{0.75}Cr_{0.25}$, doped (**f**) $Ru_{0.75-x}Cr_{0.25}Fe_x$ (**g**) $Ru_{0.75-x}Cr_{0.25}Mn_x$ and (**h**) $Ru_{0.75-x}Cr_{0.25}Mo_x$ ruthenium-rich alloys. Note that for doped systems, $x = 0.09$. The Fermi energy, $E - E_f = 0$ is taken as the zero energy.

Table 2. Calculated elastic constants C_{ij} (GPa) of undoped and doped A15 $Ru_{0.75}Cr_{0.25}$ and A15 $Cr_{0.75}Ru_{0.25}$ structure.

System	C_{11} (GPa)	C_{12} (GPa)	C_{44} (GPa)	$C_{12} - C_{44}$ (GPa)	$C' = [1/2(C_{11} - C_{12})]$ (GPa)
$Cr_{0.75}Ru_{0.25}$	459.69	169.29	97.71	72.04	145.20
$Cr_{0.75-x}Ru_{0.25}Mn_x$	417.44	131.48	99.07	32.41	142.98
$Cr_{0.75-x}Ru_{0.25}Fe_x$	424.72	169.70	87.49	82.21	127.51
$Cr_{0.75-x}Ru_{0.25}Mo_x$	518.06	197.63	103.14	94.49	160.22
$Ru_{0.75}Cr_{0.25}$	410.13	210.45	73.81	136.64	99.84
$Ru_{0.75-x}Cr_{0.25}Mn_x$	348.33	216.73	73.08	143.65	65.80
$Ru_{0.75-x}Cr_{0.25}Fe_x$	343.22	190.93	96.57	94.36	76.15
$Ru_{0.75-x}Cr_{0.25}Mo_x$	426.70	210.38	91.71	118.67	108.16

flat with the peaks becoming more flattened upon doping in the case of the later. The flat peaks in the Ru_3Cr indicate that the electronic states in the system are more localized. Comparing the position of the Fermi level in both the Ru_3Cr and Cr_3Ru systems, it is seen that the Fermi level falls within a clearly defined pseudogap in the case of doped Ru_3Cr systems, whereas in Cr_3Ru, the Fermi level falls in the anti-bonding states, in agreement with previous studies by Ravindran and Asokamani [23]. This result explains the calculated heat of formation results discussed in section 3.1 above, where the effect of doping is more pronounced in the Ru_3Cr systems compared to the Cr_3Ru systems. Further, the observed trend in the stability of transition metal-doped Cr_3Ru and Ru_3Cr systems can also be explained by the depth of the pseudogap, where the depth of the pseudogap is largest in Mn-doped Ru_3Cr system. In the case of Mn-doped Cr_3Ru system, the pseudogap falls within a shoulder peak, hence, the system is less stable.

4. Mechanical properties

4.1 *Mechanical stability*

Elastic constants play a vital role in determining the mechanical deformation of a material under external load and structural stability [24,25]. It is known that elastic constants depend on the type of lattice, for example, cubic, tetragonal, orthorhombic and monoclinic crystals have three, six, nine and thirteen independent elastic constants, respectively [26]. For the cubic crystals of Cr_3Ru and Ru_3Cr studied herein, the independent elastic constants are C_{11}, C_{12} and C_{44}. Table 2 and figure 4 present the elastic constants of Mn-, Fe- and Mo-doped Cr_3Ru and Ru_3Cr cubic ternary alloys at 0.09 atm% dopant concentration. The elastic constants of the undoped systems are also shown for comparison.

Bohr stability criteria [27,28] states that a system is mechanically stable if

$$C_{44} > 0,\ C_{11} > |C_{12}| \text{ and } C_{11} + 2C_{12} > 0. \quad (3)$$

It is noted that both the doped and undoped systems have elastic constants >0, hence, these structures are elastically stable, which is consistent with the heat of formation trend (figure 2). It can be seen that C_{11} is larger than C_{12} and C_{44} in both systems with a much lower C_{12} curve close to C_{44} curve in the case of Mn-doped Cr_3Ru a result which can be attributed to their difference in stability.

The Cauchy pressure is used to describe the angular character of atomic bonding in metals and compounds, and is given by [29]

$$(C_{12} - C_{44}) < 0. \quad (4)$$

We find that all structures studied herein have positive Cauchy pressure, which indicates metallic bonding.

The present study has been extended to further calculate the bulk modulus (B), which measures the resistance of material under compression; shear modulus (G), which measures how strong the material is to resist deformation; Young's modulus (E), which predicts how stiff a material is. These moduli are approximated by Voigt [30]. The arithmetic Hill [31] approximation averages the Voigt and Reuss [30,32] approximations as:

$$B = B_H = (B_V + B_R)/2, \quad (5)$$

where

$$B = B_R = B_V = (C_{11} + 2C_{12})/3. \quad (6)$$

B_R, $B = B_H$ and B_V are the bulk moduli for Reuss, Voigt and Hill approximations.

$$G = G_H = (G_V + G_R)/2, \quad (7)$$

where

$$G_V = (C_{11} - C_{12} + 3C_{44})/5, \quad (8)$$

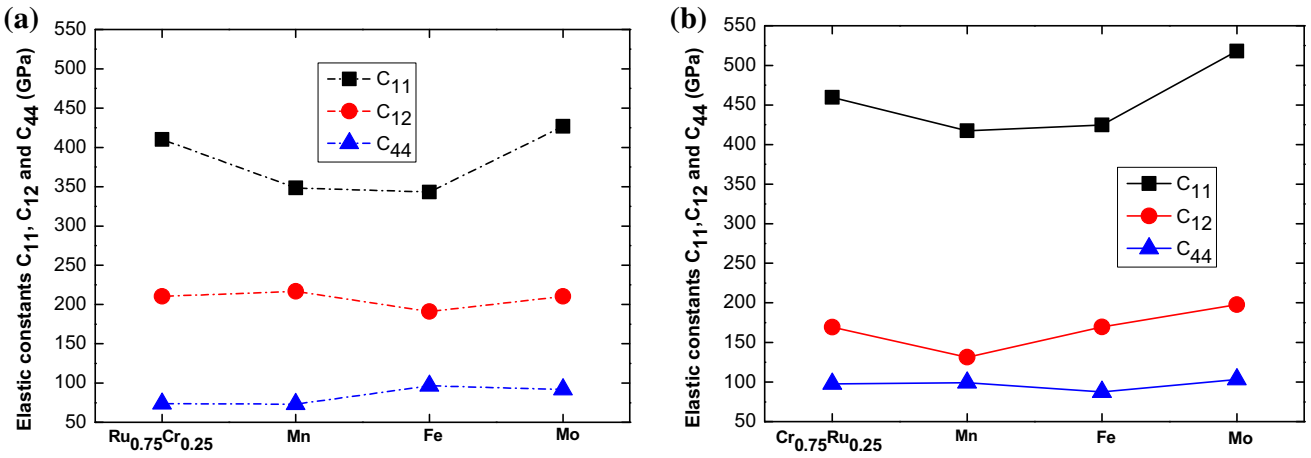

Figure 4. Elastic constants of (**a**) Ru_3Cr and (**b**) Cr_3Ru doped with Mn, Fe and Mo calculated at a dopant concentration of 0.09 atm%.

Table 3. Calculated bulk (B), shear (G) and Young's (E) of Voigt, Reuss and Hill, bulk to shear ratio, Poisson's ratio, density (g cm^{-3}), anisotropy factor (A), melting temperature (T_m) and Vicker's hardness (H_V) of un-doped and doped structures ($x = 0.09$ atm%).

		(B, G and E)$_{VRH}$ (GPa)								
System	Modulus	Voigt	Reuss	Hill	B_H/G_H	Poisson (υ)	Density (g cm^{-3})	(A)	T_m (K)	H_V (GPa)
$Cr_{0.75}Ru_{0.25}$	Bulk	266.09	266.09	266.09						
	Shear	116.71	112.42	114.57	2.32	0.31	10.29	0.673	3269.77	8.951
	Young	300.57	300.57	300.57						
$Cr_{0.75-x}Ru_{0.25}Mn_x$	Bulk	226.80	226.80	226.80						
	Shear	116.63	112.94	114.79	1.98	0.28	9.32	0.693	3020.07	11.456
	Young	294.66	294.66	294.66						
$Cr_{0.75-x}Ru_{0.25}Fe_x$	Bulk	254.71	254.71	254.71						
	Shear	103.50	100.13	101.82	2.50	0.32	9.36	0.686	3063.10	7.226
	Young	269.54	269.54	269.54						
$Cr_{0.75-x}Ru_{0.25}Mo_x$	Bulk	304.44	304.44	304.44						
	Shear	125.97	120.28	123.13	2.47	0.32	11.16	0.644	3614.73	8.586
	Young	325.51	325.51	325.51						
$Ru_{0.75}Cr_{0.25}$	Bulk	277.01	277.01	277.01						
	Shear	84.22	82.40	83.31	3.33	0.36	9.33	0.739	2976.87	3.518
	Young	227.16	227.16	227.16						
$Ru_{0.75-x}Cr_{0.25}Mn_x$	Bulk	260.60	260.60	260.60						
	Shear	70.17	70.00	70.09	3.71	0.38	8.45	1.111	2611.63	2.170
	Young	192.97	192.97	192.97						
$Ru_{0.75-x}Cr_{0.25}Fe_x$	Bulk	241.69	241.69	241.69						
	Shear	88.40	87.21	87.81	2.75	0.34	8.49	1.268	2581.43	5.386
	Young	234.97	234.97	234.97						
$Ru_{0.75-x}Cr_{0.25}Mo_x$	Bulk	282.49	282.49	282.49						
	Shear	98.29	97.65	97.97	2.88	0.34	10.11	0.848	3074.80	5.467
	Young	263.45	263.45	263.45						

and

$$G_R = (5(C_{11} - C_{12})C_{44})/(4C_{44} + 3(C_{11} - C_{12})), \quad (9)$$

$$E = (9BG)/(3B + G), \quad (10)$$

$$\upsilon = (3B - 2G)/(2(3B + G)), \quad (11)$$

where G_R and G_V are the Reuss and Voigt bounds, respectively [33]. G_H, B_H, E and υ are shear modulus, bulk modulus, Young's modulus and Poisson's ratio, respectively.

The bulk, shear and Young's moduli, B/G ratio and Poisson's ratio of the A15 $Cr_{0.75}Ru_{0.25}$ and A15 $Ru_{0.75}Cr_{0.25}$ systems doped with Mn, Fe and Mo are shown in table 3.

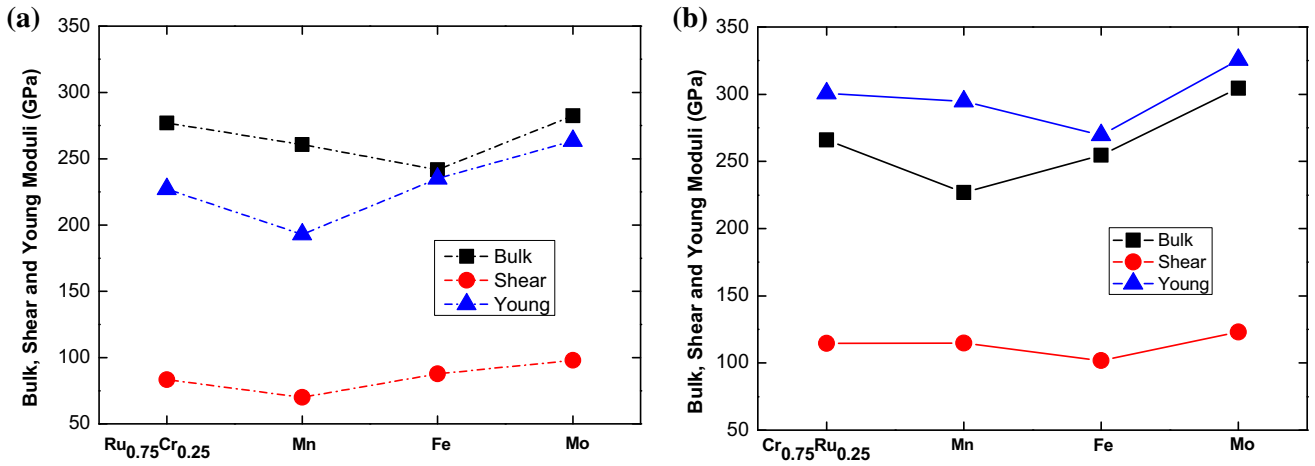

Figure 5. Bulk, shear and Young's moduli of (**a**) Ru_3Cr and (**b**) Cr_3Ru doped with Mn, Fe and Mo calculated at dopant concentration of 0.09 atm%.

It is well known that the strength of the material and hardness are related to Young's, bulk and shear moduli [25]. The general trend is that the larger the modulus, the harder the material. Figure 5 shows the bulk, shear and Young's moduli of Mn, Fe and Mo-doped $Cr_{0.75}Ru_{0.25}$ and $Ru_{0.75}Cr_{0.25}$ systems at 0.09 atm% concentration (moduli of the undoped systems is also shown for comparison). It can be seen that $Cr_{0.75}Ru_{0.25}$ and $Ru_{0.75}Cr_{0.25}$ doped with Mo has the largest bulk, shear and Young's moduli, which can be attributed to the strong stress–strain effects caused by Mo dopant in the structure.

The ratio of bulk to shear modulus (B/G) as proposed by Pugh [34] links the plastic properties of metals with their elastic moduli. If B/G>1.75, the material is ductile, otherwise, it is brittle. We find that the B/G ratios of all the structures are >1.75 (figure 6), suggesting ductility of the structures. In particular, Cr_3Ru is more ductile upon doping with Fe and Mo, while Ru_3Cr is more ductile when doped with Mn.

Considering the Poisson's ratio, it is apparent that the $Ru_{0.75}Cr_{0.25}$ and $Cr_{0.75}Ru_{0.25}$ systems doped with Mn, Fe and Mo possess similar trend, as indicated in figure 6. However, from table 3, it is seen that $Ru_{0.75-x}Cr_{0.25}Mn_x$ has a large Poisson's ratio of 0.38, while $Cr_{0.75-x}Ru_{0.25}Mn_x$ has the least Poisson's ratio of 0.28.

To further characterize the mechanical properties of the Cr_3Ru and Ru_3Cr alloys, we evaluated their hardness character (which measures the resistance to deformation under an applied force) using the Vickers hardness criteria given by Chen *et al* [35]:

$$H_V = 2(K^2G)^{0.585} - 3, \tag{12}$$

where K is G/B. The predicted hardness values are given in table 3. It can be seen that $Cr_{0.75}Ru_{0.25}$ possess higher hardness values compared to Fe and Mo doped $Cr_{0.75}Ru_{0.25}$ structure. Moreover, hardness enhancement is visible from $Cr_{0.75}Ru_{0.25}$ to Mn-doped $Cr_{0.75}Ru_{0.25}$. On the other hand, hardness increased from $Ru_{0.75}Cr_{0.25}$ to Fe and Mo-doped $Ru_{0.75}Cr_{0.25}$.

4.2 *Density*

Density of the system characterizes the lightness or heaviness of a material. Lightweight materials are best suited for elevated temperature applications such as in the aerospace industry where low density is a major requirement. We have therefore calculated the densities of the Cr_3Ru and Ru_3Cr systems to determine their applicability in such applications. The density (in g cm^{-3}) of material is given by:

$$\rho^{\text{cal}} = \left[\frac{M_W * N}{\text{Vol} * A_0}\right], \tag{13}$$

where Vol is the volume of the cell measured in $Å^3$, M_W the average molecular weight of the total elements, N the number of atoms and A_0 the Avogadro's number in atom per mole (6.022×10^{23}). The calculated densities of both doped and undoped $Ru_{0.75}Cr_{0.25}$ and $Cr_{0.75}Ru_{0.25}$ are also listed in table 3 and figure 6. We find that doping these systems with Fe and Mn considerably lowers their densities. These densities are in the range of previously obtained densities for Ni_3Al (6.14 g cm^{-3}) and Ru_3Al (7.55 g cm^{-3}) [36].

4.3 *Melting temperature*

We have further considered the effect of dopants on the melting temperature (T_m) of the Ru_3Cr and Cr_3Ru systems to assess their applicability in high temperature structural applications. For cubic systems, the melting temperature can be estimated from the elastic constants [36–39] as follows:

$$T_m = 553\ \text{K} + \left(\frac{591\ \text{K}}{\text{Mbar}}\right) * C_{11}\ (\text{Mbar}) \pm 300\ \text{K}, \tag{14}$$

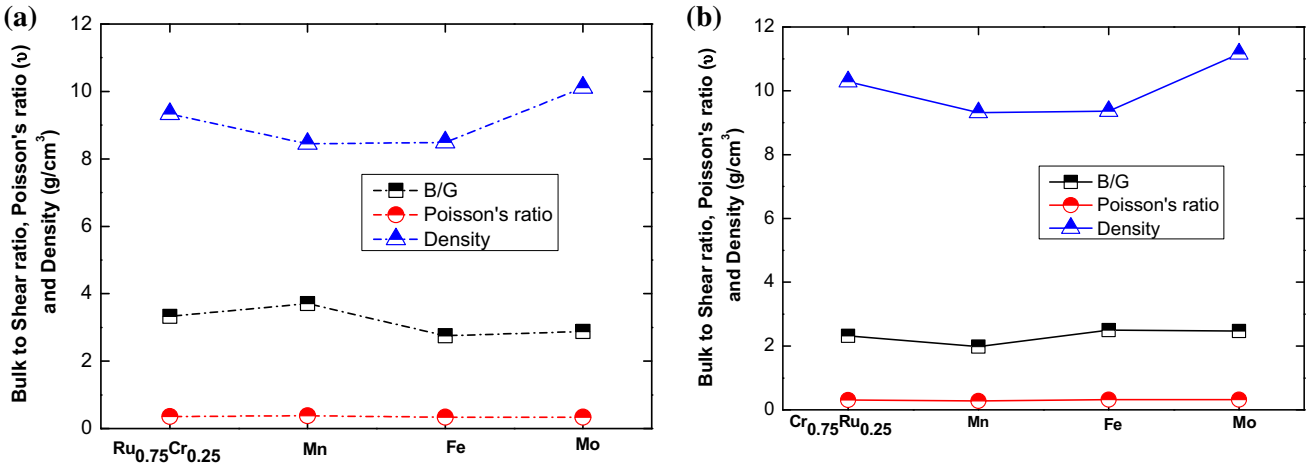

Figure 6. Bulk to shear ratio, Poisson's ratio and density (g cm^{-3}) of (**a**) $Ru_{0.75}Cr_{0.25}$ and (**b**) $Cr_{0.75}Ru_{0.25}$ doped with Mn, Fe and Mo calculated at a dopant concentration of 0.09 atm%.

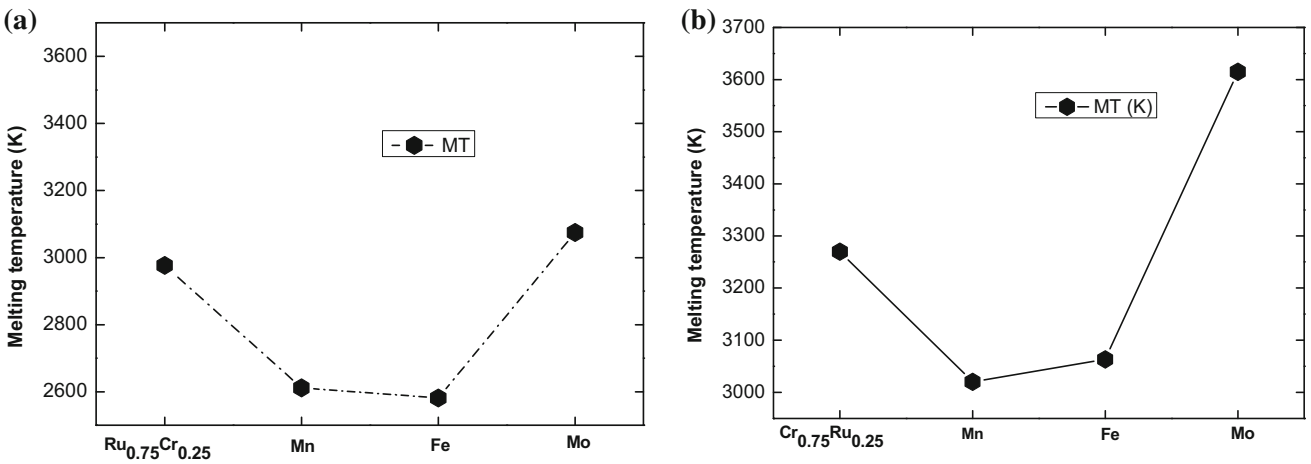

Figure 7. Melting temperatures (K) of (**a**) Ru_3Cr and (**b**) Cr_3Ru doped with Mn, Fe and Mo calculated at a dopant concentration of 0.09 atm%.

where M is in mega bar and K = kelvin. The predicted T_m are shown in table 3 and figure 7. We find that Mo enhances the melting temperature of both the Ru_3Cr and Cr_3Ru, while Mn and Fe lower their melting temperature with the melting point of Mo doped $Cr_{0.75}Ru_{0.25}$ being the highest at >3600 K. Our predicted melting point temperatures are much higher than those previously reported for Ni_3Al (1668 ± 300 K) [37] and are comparable to that of Ru_3Al (2136 ± 300 K) [36].

4.4 *Elastic anisotropy*

The elastic anisotropy (A) has been evaluated to characterize the micro-cracks in doped $Ru_{0.75}Cr_{0.25}$ and $Cr_{0.75}Ru_{0.25}$ systems [40]. The anisotropy factor is calculated as:

$$A = \left(\frac{2C_{44}}{C_{11} - C_{12}}\right). \tag{15}$$

Isotropic materials have an anisotropic factor $A = 1$, but if A has any value greater or less than one, it implies that the material is anisotropic. From table 3, it is seen that the anisotropic factor for $Ru_{0.75-x}Cr_{0.25}Mn_x$ (1.111) is close to unity, implying that this material system is slightly isotropic, whilst all the other materials are anisotropic.

5. Conclusion

Ab initio density functional theory calculations have been performed to study the electronic and elastic properties of transition metal doped A15 Ru_3Cr and A15 Cr_3Ru intermetallic structures. The calculated equilibrium lattice constants of these alloys are in agreement with previous results. The calculated heat of formation indicate that doping these systems with transition metal atoms considerably lower their

thermodynamic stability with Mn-doped $Ru_{0.75}Cr_{0.25}$ and $Cr_{0.75}Ru_{0.25}$ being the most favourable. The calculated DOS is used to explain the trends in chemical stability. Further, the elastic constants C_{11}, C_{12} and C_{44} show that the systems are elastically stable. The ratio of B/G shows that the undoped and doped structures are ductile with metallic bonding due to positive Cauchy pressures. The calculated melting point of Mo-doped Cr_3Ru is >3600 K, which is much higher than that of the currently used Ni_3Al system. These results show doping Cr_3Ru and Ru_3Cr intermetallic alloys with transition metal atoms enhance both their thermodynamic and mechanical stabilities, making them suitable for high-temperature structural applications.

Acknowledgements

This work was supported by the National Research Foundation (Grant No. 96897) and UNISA Masters and Doctoral Bursary. The computational work was performed using high-performance computing (HPC) facilities at the University of South Africa and the Centre for High-Performance Computing (CHPC) at the CSIR, South Africa.

References

[1] Sims C T, Stoloff N S and Hagel W C 1987 *Superalloys II* (New York: Wiley)
[2] Yamabe Y, Koizumi Y, Murakami H, Ro Y, Maruko T and Harada H 1996 *Scr. Mater.* **35** 211
[3] Cornish L A, Hohls J, Hill P J, Prins S, Süss R and Compton D N 2002 *J. Min. Metall. B: Metall.* **38** 197
[4] Cornish L A, Fischer B and Völkl R 2003 *MRS Bull.* **28** 632
[5] Liao P K, Spear K E and Massalski T B 1990 *Binary alloy phase diagrams* (Ohio: ASM Int. Mater. Park) vol 1, p 557
[6] Süss R, Cornish L A and Glatzel U 2004 *CALPHAD XXXIII Progr. Abstr.* **34**
[7] Wopersnow W and Raub C J 1979 *Metallics* **33** 1261
[8] Venkatraman B M and Neumann J P 1987 *Bull. Alloy Phase Diagrams* **8** 109
[9] Chakravorty S and West D R F 1984 *Met. Sci.* **18** 207
[10] Milman V, Winkler B, White J A, Pickard C J, Payne M C and Akhmatskaya E V 2000 *Int. J. Quantum Chem.* **77** 895
[11] Zhao J-C 2004 *J. Mater. Sci.* **39** 3913
[12] Perdew J P and Wang Y 1992 *Phys. Rev. B* **45** 13244
[13] Perdew J, Burke K and Ernzerhof M 1996 *Phys. Rev. Lett.* **77** 3865
[14] Vanderbilt D 1990 *Phys. Rev. B* **41** 7892
[15] Monkhorst H J and Pack J D 1976 *Phys. Rev. B* **13** 5188
[16] Medvedeva N I and Ivanovskii A L 2014 *Nanosyst.: Phys. Chem. Math.* **5** 486
[17] Tibane M M 2011 *Phase stability study of Pt–Cr and Ru–Cr binary alloys* (Turfloop Campus: University of Limpopo)
[18] Gelatt Jr C D, Williams A R and Moruzzi V L 1983 *Phys. Rev. B* **27** 2005
[19] Pasturel A, Colinet C and Hicter P 1985 *Phys. B + C* **132** 177
[20] Hong T, Watson-Yang T J, Guo X-Q, Freeman A J, Oguchi T and Xu J 1991 *Phys. Rev. B* **43** 1940
[21] Xu J and Freeman A J 1991 *J. Mater. Res.* **6** 1188
[22] Xu J-H, Oguchi T and Freeman A J 1987 *Phys. Rev. B* **36** 4186
[23] Ravindran P and Asokamani R 1997 *Bull. Mater. Sci.* **20** 613
[24] Jhi S-H, Ihm J, Louie S G and Cohen M L 1999 *Nature* **399** 132
[25] Clerc D G 1998 *J. Mater. Sci. Lett.* **17** 1461
[26] Mehl M J, Klein B M and Papaconstantopoulos D A 1994 *Intermetallic compounds: principles and applications* (London: Wiley) vol 1, p 195
[27] Born M 1940 in *Mathematical Proceedings of the Cambridge Philosophical Society*, vol 36, p 160
[28] Fedorov F I 2013 *Theory of elastic waves in crystals* (London, UK: Springer Science & Business Media)
[29] Pettifor D G 1992 *Mater. Sci. Technol.* **8** 345
[30] Voigt W 1928 *Lehrbuch der kristallphysik* (Teubner Leipzig) vol 962
[31] Hill R 1952 *Proc. Phys. Soc.* **65** 349
[32] Reuss A 1929 *Z. Angew. Math. Mech.* **9** 49
[33] Vitos L 2007 *Computational quantum mechanics for materials engineers: the EMTO method and applications* (London, UK: Springer Science & Business Media)
[34] Pugh S F 1954 *London, Edinburgh, Dublin Philos. Mag. J. Sci.* **45** 823
[35] Chen X-Q, Niu H, Li D and Li Y 2011 *Intermetallics* **19** 1275
[36] Popoola A I and Lowther J E 2014 *Int. J. Mod. Phys. B* **28** 1450066
[37] Skinner D J and Zedalis M 1988 *Scr. Metall.* **22** 1783
[38] Fine M E, Brown L D and Marcus H L 1984 *Scr. Metall.* **18** 951
[39] Blackman M 1951 *London, Edinburgh, Dublin Philos. Mag. J. Sci.* **42** 1441
[40] Tvergaard V and Hutchinson J W 1988 *J. Am. Ceram. Soc.* **71** 157